

Supporting Information:

A critical review on the multiple roles of Mn in stabilizing and destabilizing soil organic matter

by

Hui Li¹, Fernanda Santos¹, Kristen Butler², Elizabeth Herndon^{1,2*}

¹*Environmental Sciences Division, Oak Ridge National Laboratory, Oak Ridge, TN 37831*

²*Department of Earth and Planetary Sciences, College of Arts & Sciences, University of Tennessee, Knoxville, TN 37996*

*Corresponding author: Elizabeth Herndon; Email: herndonem@ornl.gov

Submitted to *Environmental Science & Technology*

2021

The supplementary information (12 pages) contains additional text describing manganese geochemistry in soils for section 2.1 and data compilation for section 6, one supplementary figure and three supplementary tables. Tables S2 and S3 are included as an electronic appendix (*.xlsx).

Manganese oxidation and mineral transformation pathways

The majority of naturally present Mn-oxides are formed during Mn(II) oxidation, which involves both enzymatic and mineral-catalyzed processes, and subsequent transformation of initial products (Figure S1).⁷⁻⁹ Microbially mediated Mn(II) oxidation by bacteria (e.g. *Pseudomonas putida*, *Leptothrix discophora* SP6) and fungi (e.g. *Plectosphaerella cucumerina* strain DS2psM2a2) generates a poorly crystalline phyllo-manganate phase similar to birnessite.^{8,25-27} This initially formed phyllo-manganate contains numerous vacancies but later converts to more ordered phases, e.g., todorokite and triclinic birnessite, mediated by various types of Mn(II)-oxidizing Ascomycete fungi.²⁶ Abiotic Mn(II) oxidation is another important and well-studied pathway for Mn-oxide formation (Figure S1). Aqueous Mn(II) oxidation by dissolved O₂ is thermodynamically unfavorable (at pH<8) and kinetically hindered due to high activation energy of the reaction.^{4,30,31} The oxidation products of Mn(II) by O₂ vary at different pH conditions; e.g., Mn(II) is oxidized to manganite (γ -MnOOH) at pH 7.5, to a mixture of feitknechtite (β -MnOOH), groutite (α -MnOOH) and manganite at pH 8, and to hausmannite (Mn₃O₄) at pH 9.³² Abiotic processes also influence mineral transformation over time. Hexagonal birnessite transforms to ramsdellite (R-MnO₂; pH 2.4), cryptomelane (KMn₈O₁₆; pH 4), and groutite (pH 6) in the presence of aqueous Mn(II),³³ or converts to feitknechtite and eventually manganite or hausmannite at higher pH (7 – 8.5).^{30,34} Hausmannite can also transform to manganite at pH 5–9 under anoxic conditions.³⁵ Mn(III)-oxides, e.g., hausmannite and manganite, are susceptible to proton-promoted disproportionation reactions that form MnO₂ precipitates such as birnessite, ramsdellite, nsutite (γ -MnO₂), and pyrolusite (β -MnO₂).^{35,36}

Mineral surfaces, such as Fe-oxides and Mn-oxides, also catalyze Mn(II) oxidation via interfacial catalysis and/or electrochemical reactions to form more Mn-oxide phases,^{32,41,42} at rates equivalent to or faster than biological oxidation.^{9,43} Abiotic Mn(II) oxidation by the Fe-oxide goethite (FeOOH) can form a mixture of hausmannite, groutite, feitknechtite and/or manganite at neutral or alkaline conditions, which are then transformed to more stable phases such as manganite.⁴² Similarly, Mn(II) oxidation on ferrihydrite surfaces can generate manganite, hausmannite, and/or birnessite at pH 6.5 to 9.³² Mn(II) oxidation by semiconductive Fe-oxides, such as ferrihydrite and goethite, follows an electrochemical pathway, i.e., electron transfer within the Mn(II)-conduction band of Fe-oxides–O₂ complexes.⁴¹ This oxidation process is highly dependent on pH conditions and mineral surface properties (e.g. semiconductivity and particle size).

Additional notes on assessing Mn-C stabilization and destabilization potential.

Our efforts to quantify stabilization and destabilization of organic compounds by Mn-oxides are complicated by data availability. For example, in order to properly assess stabilization and destabilization, it is necessary to quantify time-dependent 1) loss of an organic constituent from solution; 2) presence of that constituent in the solid-phase (adsorption); 3) presence of degradation products in solution, and in the solid-phase. This information should be coupled with quantification of solution and solid-phase Fe(II) and Mn(II) to assess net metal reduction; however, no studies fully quantify these factors. Taking Mn as an example, many studies report the release of aqueous Mn(II) into solution as an indicator of reductive dissolution of Mn(III/IV)-oxides coupled to carbon oxidation. However, aqueous Mn(II) release into solution is insufficient to quantify parallel C oxidation because 1) Mn(II) can sorb to or persist in the oxide surface,^{44, 45} and 2) sorbed Mn(II) can re-oxidize to Mn (III/IV) on the mineral surface and serve as a catalyst for carbon oxidation.⁴⁶ In a mixed-phase system, solubilized Mn(II) can be oxidized by Fe(III)-oxide surfaces⁴². Organic matter sorption to the mineral surface is typically quantified by C loss from solution; however, these interpretations are also problematic given that 1) changes in dissolved organic C concentration cannot capture C transformation reactions (sorption, reaction, release back into solution, and 2) C loss from solution may also result from CO₂ loss during decarboxylation reactions. Additional quantification of C gain in the solid-phase would complete C mass balance, although many studies only report qualitative characterization of solid-phase products. The most complete assessments of Mn-C interactions come from studies that track the removal of individual compounds and the formation of their degradation products during reaction with Mn-oxides. Evaluating a broad suite of these compounds indicate the range of expected behaviors, although do not demonstrate how Mn-oxides will react with natural organic matter that contains a complexity of poorly studied compounds.

Reactive interactions are typically represented by either the disappearance of a reactive organic compound or the increase in reduced metals in solution (e.g., Mn²⁺, Fe²⁺). The disappearance of one reactive organic compound is represented by one C atom within that molecule. Similarly, the production of either one reduced Mn²⁺ or two reduced Fe²⁺ atoms is assumed to equate to the transformation of one molecule, represented by one C atom, although the exact stoichiometry can vary. Rates are typically reported as the initial linear rates of reaction, and spontaneous degradation reactions following the initial reaction between the organic compound and metal oxide are not considered. Reactions are limited to interactions between organic molecules with mineral surfaces and exclude solution reactions involving organic-Mn(III) complexes and Fe-mediated Fenton reactions, as well as light-mediated reductive dissolution (e.g., reductive dissolution of Fe(III)-oxides by oxalate).

References

1. Turekian, K. K.; Wedepohl, K. H., Distribution of the elements in some major units of the Earth's crust. *Geol. Soc. Am. Bull.* **1961**, *72*, 175-192.
2. EPA, U. S., Health effects support document for manganese. *U.S. Environmental Protection Agency, Office of Water. EPA. EPA-822-R-03-003. Washington, D.C.* **2003**.
3. Hochella, M. F. J.; Kasama, T.; Putnis, A.; Putnis, C. V.; Moore, J. N., Environmental important, poorly crystalline Fe/Mn hydrous oxides: Ferrihydrite and a possibly new vernadite-like mineral from the Clark Fork River Superfund Complex. *Am. Mineral.* **2005**, *90*, 718-724.
4. Morgan, J. J., Kinetics of reaction between O₂ and Mn(II) species in aqueous solutions. *Geochim. Cosmochim. Acta* **2005**, *69*, 35-48.
5. Post, J. E., Manganese oxide minerals: Crystal structures and economic and environmental significance. *Proc. Natl. Acad. Sci. USA* **1999**, *96*, 3447-3454.
6. Feng, X. H.; Zhai, L. M.; Tan, W. F.; Liu, F.; He, J. Z., Adsorption and redox reactions of heavy metals on synthesized Mn oxide minerals. *Environ. Pollut.* **2007**, *147*, 366-373.
7. Tebo, B. M.; Bargar, J. R.; Clement, B. G.; Dick, G. J.; Murray, K. J.; Parker, D.; Verity, R.; Webb, S. M., Biogenic manganese oxides: Properties and mechanisms of formation. *Annu. Rev. Earth Planet. Sci.* **2004**, *32*, 287-328.
8. Hansel, C. M.; Learman, D. R., Chapter eighteen: Geomicrobiology of manganese. *Ehrlich's Geomicrobiology, Boca Raton, CRC Press* **2015**, 401-452.
9. Learman, D. R.; Wankel, S. D.; Webb, S. M.; Martinez, N.; Madden, A. S.; Hansel, C. M., Coupled biotic-abiotic Mn(II) oxidation pathway mediates the formation and structural evolution of biogenic Mn oxides. *Geochim. Cosmochim. Acta* **2011**, *75*, 6048-6063.
10. Spiro, T. G.; Bargar, J. R.; Sposito, G.; Tebo, B. M., Bacteriogenic manganese oxides. *Acc. Chem. Res.* **2010**, *43*, 2-9.
11. Hansel, C. M., Manganese in marine microbiology. *Adv. Microb. Physiol.* **2017**, *70*, 37-83.
12. Butterfield, C. N.; Soldatova, A. V.; Lee, S.-W.; Spiro, T. G.; Tebo, B. M., Mn(II,III) oxidation and MnO₂ mineralization by an expressed bacterial multicopper oxidase. *Proc. Natl. Acad. Sci. USA* **2013**, *110*, 11731-11735.
13. Andeer, P. F.; Leadbetter, J. R.; McIlvin, M.; Dunn, J. A.; Hansel, C. M., Extracellular haem peroxidases mediate Mn(II) oxidation in a marine *Roseobacter* bacterium via superoxide production. *Environ. Microbiol.* **2015**, *17*, 3925-3936.
14. Tang, Y.; Zeiner, C. A.; Santelli, C. M.; Hansel, C. M., Fungal oxidative dissolution of the Mn(II)-bearing mineral rhodochrosite and the role of metabolites in manganese oxide formation. *Environ. Microbiol.* **2013**, *15*, 1063-1077.
15. Chaput, D. L.; Jowler, A. J.; Seo, O.; Duhn, K.; Hansel, C. M.; Santelli, C. M., Mn oxide formation by phototrophs: Spatial and temporal patterns, with evidence of an enzymatic superoxide-mediated pathway. *Sci. Rep.* **2019**, *9*, 18244.
16. van Genuchten, C. M.; Peña, J., Mn(II) oxidation in fenton and fenton type systems: Identification of reaction efficiency and reaction products. *Environ. Sci. Technol.* **2017**, *51*, 2982-2991.
17. Jung, H.; Chadha, T. S.; Kim, D.; Biswas, P.; Jun, Y.-S., Photochemically assisted fast abiotic oxidation of manganese and formation of \square -MnO₂ nanosheets in nitrate solution. *Chem. Commun.* **2017**, *53*, 4445.

18. Nico, P. S.; Anastasio, C.; Zasoski, R. J., Rapid photo-oxidation of Mn(II) mediated by humic substances. *Geochim. Cosmochim. Acta* **2002**, *66*, 4047-4056.
19. Xu, X.; Li, Y.; Li, Y.; Lu, A.; Qiao, R.; Liu, K.; Ding, H.; Wang, C., Characteristics of desert varnish from nanometer to micrometer scale: A photo-oxidation model on its formation. *Chem. Geol.* **2019**, *522*, 55-70.
20. Hofrichter, M., Review: lignin conversion by manganese peroxidase (MnP). *Enzyme and Microbial Technology* **2002**, *30*, (4), 454-466.
21. Hansel, C. M.; Zeiner, C. A.; Santelli, C. M.; Webb, S. M., Mn(II) oxidation by an ascomycete fungus is linked to superoxide production during asexual reproduction. *Proc. Natl. Acad. Sci. USA* **2012**, *109*, 12621-12625.
22. Bohu, T.; Santelli, C. M.; Akob, D. M.; Neu, T. R.; Ciobota, V.; Rösch, P.; Popp, J.; Nietzsche, S.; Küsel, K., Characterization of pH dependent Mn(II) oxidation strategies and formation of a bixbyite-like phase by *Mesorhizobium australicum* T-G1. *Front. Microbiol.* **2015**, *6*, 734.
23. Yu, H.; Leadbetter, J. R., Bacterial chemolithoautotrophy via manganese oxidation. *Nature* **2020**, *583*, 453-458.
24. Ehrlich, H. L.; Salerno, J. C., Energy coupling in Mn²⁺ oxidation by a marine bacterium. *Arch. Microbiol.* **1990**, *154*, 12-17.
25. Saratovsky, I.; Wightman, P. G.; Pastén, P. A.; Gaillard, J.; Poeppelmeier, K. R., Manganese oxides: Parallels between abiotic and biotic structures. *J. Am. Chem. Soc.* **2006**, *128*, 11188-11198.
26. Santelli, C. M.; Webb, S. M.; Dohnalkova, A. C.; Hansel, C. M., Diversity of Mn oxides produced by Mn(II)-oxidizing fungi. *Geochim. Cosmochim. Acta* **2011**, *75*, 2762-2776.
27. Villalobos, M.; Lanson, B.; Manceau, A.; Toner, B.; Sposito, G., Structural model for the biogenic Mn oxide produced by *pseudomonas putida*. *Am. Mineral.* **2006**, *91*, 489-502.
28. Lovley, D. R.; Phillips, E. J., Novel mode of microbial energy metabolism: Organic carbon oxidation coupled to dissimilatory reduction of iron or manganese. *Appl. Environ. Microbiol.* **1988**, *54*, 1472-1480.
29. Lin, H.; Szeinbaum, N. H.; DiChristina, T. J.; Taillefert, M., Microbial Mn(IV) reduction requires an initial one-electron reductive solubilizaiton step. *Geochim. Cosmochim. Acta* **2012**, *99*, 179-192.
30. Elzinga, E. J., Reductive transformation of birnessite by aqueous Mn(II). *Environ. Sci. Technol.* **2011**, *45*, 6366-6372.
31. Luther III, G. W., The role of one- and two-electron transfer reactions in forming thermodynamically unstable intermediates as barriers in multi-electron redox reactions. *Aqua. Geochim.* **2010**, *16*, 395-420.
32. Wang, X.; Lan, S.; Zhu, M.; Ginder-Vogel, M.; Yin, H.; Liu, F.; Tan, W.; Feng, X., The presence of ferrihydrite promotes abiotic formation of manganese (oxyhydr)oxides. *Soil Sci. Soc. Am. J.* **2015**, *79*, 1297-1305.
33. Tu, S.; Racz, G. J.; Goh, T. B., Transformation of synthetic birnessite as affected by pH and manganese concentration. *Clays Clay Mineral.* **1994**, *42*, 321-330.
34. Lefkowitz, J. P.; Rouff, A. A.; Elzinga, E. J., Influence of pH on the reductive transformation of birnessite by aqueous Mn(II). *Environ. Sci. Technol.* **2013**, *47*, 10364-10371.
35. Luo, Y.; Tan, W.; Suib, S. L.; Qiu, G.; Liu, F., Dissolution and phase transformation processes of hausmannite in acidic aqueous systems under anoxic conditions. *Chem. Geol.* **2018**, *487*, 54-62.

36. Cornell, R. M.; Giovanoli, R., Transformation of hausmannite into birnessite in alkaline media. *Clays Clay Mineral.* **1988**, *36*, 249-257.
37. Yin, H.; Li, H.; Wang, Y.; Ginder-Vogel, M.; Qiu, G.; Feng, X.; Zheng, L.; Liu, F., Effects of Co and Ni co-doping on the structure and reactivity of hexagonal birnessite. *Chem. Geol.* **2014**, *381*, 10-20.
38. Webb, S. M.; Fuller, C. C.; Tebo, B. M.; Bargar, J. R., Determination of uranyl incorporation into biogenic manganese oxides using X-ray absorption spectroscopy and scattering. *Environ. Sci. Technol.* **2006**, *40*, 771-777.
39. Ruiz-Garcia, M.; Villalobos, M.; Voegelin, A.; Pi-Puig, T.; Martínez-Villegas, N.; Göttlicher, J., Transformation of hexagonal birnessite upon reaction with thallium(I): Effects of birnessite crystallinity, pH, and thallium concentration. *Environ. Sci. Technol.* **2021**, *55*, 4862-4870.
40. Zhang, T.; Liu, L.; Tan, W.; Suib, S. L.; Qiu, G., Formation and transformation of manganese(III) intermediates in the photochemical generation of manganese(IV) oxide minerals. *Chemosphere* **2020**, *262*, 128082.
41. Lan, S.; Wang, X.; Xiang, Q.; Yin, H.; Tan, W.; Qiu, G.; Liu, F.; Zhang, J.; Feng, X., Mechanisms of Mn(II) catalytic oxidation on ferrihydrite surfaces and the formation of manganese (oxyhydr)oxides. *Geochim. Cosmochim. Acta* **2017**, *211*, 79-96.
42. Ma, D.; Wu, J.; Yang, P.; Zhu, M., Coupled Manganese Redox Cycling and Organic Carbon Degradation on Mineral Surfaces. *Environ Sci Technol* **2020**, *54*, (14), 8801-8810.
43. Madden, A. S.; Hochella, M. F. J., A test of geochemical reactivity as a function of mineral size: Manganese oxidation promoted by hematite nanoparticles. *Geochim. Cosmochim. Acta* **2005**, *69*, 389-398.
44. Stone, A. T.; Ulrich, H., Kinetics and Reaction Stoichiometry in the Reductive Dissolution of Manganese(IV) Dioxide and Co(III) Oxide by Hydroquinone. *J Colloid Interface Sci* **1989**, *132*, (2), 509-522.
45. Stuckey, J. W.; Goodwin, C.; Wang, J.; Kaplan, L. A.; Vidal-Esquivel, P.; Beebe Jr., T. P.; Sparks, D. L., Impacts of hydrous manganese oxide on the retention and lability of dissolved organic matter. *Geochem. Trans.* **2018**, *19*, 6.
46. Barrett, K. A.; McBride, M. B., Oxidative Degradation of Glyphosate and Aminomethylphosphonate by Manganese Oxide. *Environmental Science and Technology* **2005**, *39*, 9223-9228.

Figure S1. A flow chart showing select pathways for Mn-oxide formation and transformation, including biogenic (mediated by multicopper oxidase, haem peroxidase and microbially generated superoxide) and abiotic (oxidized by O₂ with and without mineral surfaces catalysis) reactions described in the text. Simplified polyhedral representation of the crystal structures of Mn-oxides are illustrated below each name. Cations present in interlayer or tunnels were omitted for simplicity. Mn^{IV}O₆ octahedra, Mn^{III}O₆ octahedra and Mn^{II}O₄ tetrahedra are shown as green, grey, and purple, respectively.

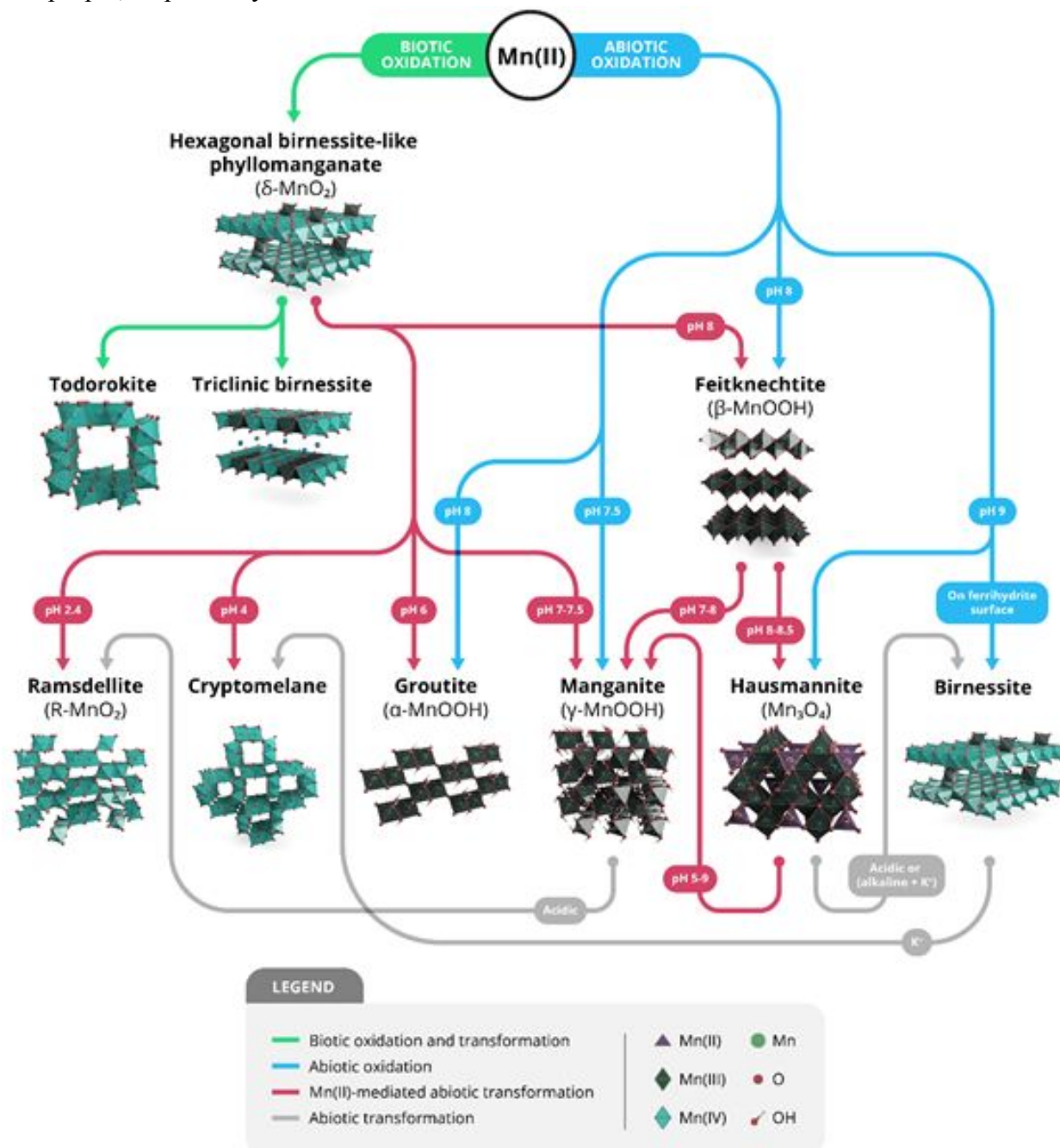


Table S1. Occurrence and properties of common Mn-oxides phases in soils and sediments

Mineral	Structure <i>Formula</i>	Occurrence ¹	Transformation	SSA ^a	PZC ^b
Lithiophorite	Layer $LiAl_2(Mn^{4+}, Mn^{3+})O_6(OH)_6$	Weathered zones of Mn deposits, acid soils, low-T hydrothermal veins		6.9 ²	
Chalcophanite	Layer $ZnMn_3O_7 \cdot 3H_2O$	Mn-bearing base metal deposits			
Birnessite	Layer $\delta-MnO_2$	Dominant in soils, desert varnishes, coatings, and ocean Mn nodules	<ul style="list-style-type: none"> • Todorokite³ • Cryptomelane (K^+)⁴ or (Mn(II), pH 4)⁵ • Nsutite (Na^+)⁴ • Ramsdellite (Mn(II), pH 2.4), groutite (Mn(II), pH 6)⁵ • Feitknechtite (Mn(II), pH 8)^{6, 7} • Manganite (Mn(II), pH 7–7.5)⁶ • Lithiophorite (Li^+ and Al^{3+}, pH 5–9)⁸ 	48.3 ⁹ 19 ¹⁰ 140 ¹¹ 15–230 ¹² 83.8±0.7 ¹³ 15.9–98.6 ¹⁴ 174.3 ¹⁵	1.75 ⁹ 1.4–4.5 ¹¹ <2 ¹³ 1.2–1.6 ¹⁶
Buserite	Layer $Na_4Mn_{14}O_{27}$	Ocean Mn nodules (before drying)	<ul style="list-style-type: none"> • Birnessite • Lithiophorite (Li^+ and Al^{3+}, pH>4)¹⁷ • Todorokite¹⁸ 	50–95 ¹⁹	
Vernadite	Layer $MnO_2 \cdot nH_2O$	Oxidized zone of Mn ore deposits, ocean Mn nodules, Mn-oxides crusts and coatings	<ul style="list-style-type: none"> • Cryptomelane²⁰ 		
Pyrolusite	Tunnel: 1×1 $\beta-MnO_2$	Low-T hydrothermal deposits	<ul style="list-style-type: none"> • Buserite (Mn(II), pH>7)¹⁷ 	4.05 ²¹ 1–2 ²²	<4.3 ²³ 7.2 ²
Ramsdellite	Tunnel: 1×2 $R-MnO_2$	Low-T hydrothermal deposits	<ul style="list-style-type: none"> • Pyrolusite (pH 2.6)²⁴ 	48.9–241.2 ²⁵	
Nsutite	Tunnel: 1×3 or 3×3 $\gamma-MnO_2$	Ore deposits and ocean Mn nodules; intergrowth between pyrolusite and ramsdellite	<ul style="list-style-type: none"> From oxidation of Mn carbonate minerals • Pyrolusite (acidic)²⁴ 	38 ²⁶	
Hollandite	Tunnel: 2×2	Oxidized Mn deposits and ores	From feldspar minerals at high pressures		^H 4.6 ²⁸
Cryptomelane	$Ba_x(Mn^{4+}, Mn^{3+})_8O_{16}$			c130.7 ⁹	^C 2.1 ⁹

Coronadite	$K_x(Mn^{4+},Mn^{3+})_8O_{16}$			c96 ²⁷	c2.0–2.1 ¹⁶
Manjiroite	$Pb_x(Mn^{4+},Mn^{3+})_8O_{16}$				
	$Na_x(Mn^{4+},Mn^{3+})_8O_{16}$				
Romanechite	Tunnel: 2×3 $(Ba, K, Mn,$ $Ca)_2(Mn^{4+},Mn^{3+})_5O_{10}$	Botryoidal masses in oxidized zones of Mn-rich deposits	• Hollandite (> 550 °C)	38±0.17 ²⁹	
Todorokite	Tunnel: 3×3 $(Na, Ca,$ $K)_x(Mn^{4+},Mn^{3+})_6O_{12}$	Oxidized zones of terrestrial Mn deposits		98.5 ⁹ 62.5 ¹⁸ 3.2 ²	3.5 ⁹ 3.5–4.0 ¹⁶
Manganite	Tunnel: 1×1; 1×2	Hydrothermal vein deposits, intimately mixed with pyrolusite	• ^M Pyrolusite at 300 °C	^M 9.5±1.4 ³⁰	^M 7.4±0.3 ³
Groutite	$\gamma\text{-}MnOOH$		• ^M Ramsdellite or nsutite (acidic) ²⁴	^M 39, 48 ²⁴	0
Feitknechtite	$\alpha\text{-}MnOOH$ $\beta\text{-}MnOOH$		• ^F Manganite (pH 7–8); Hausmannite (pH 8–8.5) ⁶		
Hausmannite	Spinel $Mn^{2+}Mn^{3+}_2O_4$	Hydrothermal and metamorphic deposits	• Birnessite (acidic ⁴ or alkaline + K^+ ³¹) • Manganite (pH 5–9) ⁴	38 ⁹ 20.4±0.8 ³⁰ 29 ³¹ 22 ⁴	>10 ³⁰

^aSpecific surface area ($m^2 g^{-1}$)

^bPoint of zero charge

References (Tables S1 and S2)

1. Post, J. E., Manganese oxide minerals: Crystal structures and economic and environmental significance. *Proc. Natl. Acad. Sci. USA* **1999**, *96*, 3447-3454.
2. Kim, J. G.; Dixon, J. B.; Chusuei, C. C.; Deng, Y. J., Oxidation of chromium(III) to (VI) by manganese oxides. *Soil Sci. Soc. Am. J.* **2002**, *66*, 306-315.
3. Santelli, C. M.; Webb, S. M.; Dohnalkova, A. C.; Hansel, C. M., Diversity of Mn oxides produced by Mn(II)-oxidizing fungi. *Geochim. Cosmochim. Acta* **2011**, *75*, 2762-2776.
4. Luo, Y.; Tan, W.; Suib, S. L.; Qiu, G.; Liu, F., Dissolution and phase transformation processes of hausmannite in acidic aqueous systems under anoxic conditions. *Chem. Geol.* **2018**, *487*, 54-62.
5. Tu, S.; Racz, G. J.; Goh, T. B., Transformation of synthetic birnessite as affected by pH and manganese concentration. *Clays Clay Mineral.* **1994**, *42*, 321-330.
6. Lefkowitz, J. P.; Rouff, A. A.; Elzinga, E. J., Influence of pH on the reductive transformation of birnessite by aqueous Mn(II). *Environ. Sci. Technol.* **2013**, *47*, 10364-10371.
7. Elzinga, E. J., Reductive transformation of birnessite by aqueous Mn(II). *Environ. Sci. Technol.* **2011**, *45*, 6366-6372.
8. Cui, H.; You, L.; Feng, X.; Tan, W.; Qiu, G.; Liu, F., Factors governing the formation of lithiophorite at atmospheric pressure. *Clays Clay Mineral.* **2009**, *57*, 353-360.
9. Feng, X. H.; Zhai, L. M.; Tan, W. F.; Liu, F.; He, J. Z., Adsorption and redox reactions of heavy metals on synthesized Mn oxide minerals. *Environ. Pollut.* **2007**, *147*, 366-373.
10. Yin, H.; Li, H.; Wang, Y.; Ginder-Vogel, M.; Qiu, G.; Feng, X.; Zheng, L.; Liu, F., Effects of Co and Ni co-doping on the structure and reactivity of hexagonal birnessite. *Chem. Geol.* **2014**, *381*, 10-20.
11. Allard, S.; Gutierrez, L.; Fontaine, C.; Croué, J.; Gallard, H., Organic matter interactions with natural manganese oxide and synthetic birnessite. *Sci. Total Envrion.* **2017**, *583*, 487-495.
12. Birkner, N.; Navrotsky, A., Thermodynamics of manganese oxides: Sodium, potassium, and calcium birnessite and cryptomelane. *Proc. Natl. Acad. Sci. USA* **2017**, *114*, E1046-E1053.
13. Chorover, J.; Amistadi, M. K., Reaction of forest floor organic matter at goethite, birnessite and smectite surfaces. *Geochim. Cosmochim. Acta* **2001**, *65*, 95-109.
14. Liu, M. M.; Cao, X. H.; Tan, W. F.; Feng, X. H.; Qiu, G. H.; Chen, X. H.; Liu, F., Structural controls on the catalytic polymerization of hydroquinone by birnessite. *Clays Clay Mineral.* **2012**, *59*, 525-537.
15. Wang, Y.; Stone, A. T., The citric acid-Mn^{III,IV}O₂(birnessite) reaction. Electron transfer, complex formation, and autocatalytic feedback. *Geochim. Cosmochim. Acta* **2006**, *70*, 4463-4476.
16. Tan, W.; Lu, S.; Liu, F.; Feng, X.; He, J.; Koopal, L. K., Determination of the point-of-zero charge of manganese oxides with different methods including an improved salt titration method. *Soil Sci.* **2008**, *173*, 277-286.
17. Yang, D.; Wang, M., Characterization and a fast method for synthesis of sub-micron lithiophorite. *Clays Clay Mineral.* **2003**, *51*, 96-101.
18. Cui, H.; Feng, X.; Tan, W.; He, J.; Hu, R.; Liu, F., Synthesis of todorokite-type manganese oxide from Cu-buserite by controlling the pH at atmospheric pressure. *Microporous Mesoporous Mater.* **2009**, *117*, 41-47.

19. Xhaxhiu, K., Synthetic birnessites and buserites as heavy metal cation traps and environmental remedies. *J. Metallomics Nanotechmol.* **2015**, *3*, 23-32.
20. Grangeon, S.; Fernandez-Martinez, A.; Warmont, F.; Gloter, A.; Marty, N.; Poulaing, A.; Lanson, B., Cryptomelane formation from nanocrystalline vernadite precursor: A high energy X-ray scattering and transmission electron microscopy perspective on reaction mechanisms. *Geochem. Trans.* **2015**, *16*, 12.
21. Petrie, L. M., Molecular interpretation for SO₂ dissolution kinetics of pyrolusite, manganite and hematite. *Appl. Geochem.* **1995**, *10*, 253-267.
22. Schaefer, M. V.; Handler, R. M.; Scherer, M. M., Fe(II) reduction of pyrolusite (β -MnO₂) and secondary mineral evolution. *Geochem. Trans.* **2017**, *18*, 7.
23. O'Reilly, S. E.; Hochella, M. F. J., Lead sorption efficiencies of natural and synthetic Mn and Fe-oxides. *Geochim. Cosmochim. Acta* **2003**, *67*, 4471-4487.
24. Ramstedt, M.; Sjöberg, S., Phase transformation and proton promoted dissolution of hydrous manganite (r-MnOOH). *Aqua. Geochem.* **2005**, *11*, 413-431.
25. Lu, B.; Chen, S.; Kawamoto, K., Direct hydrothermal synthesis of nanosized mesoporous ramsdellite manganese oxide with high surface area. *Mater. Res. Bull.* **2012**, *47*, 3619-3624.
26. Said, M. I., Akhtenskite-nsutite phases: Polymorphic transformation, thermal behavior and magnetic properties. *J. Alloys. Compd.* **2020**, *819*, 152976.
27. Li, H.; Liu, F.; Zhu, M.; Feng, X.; Zhang, J.; Yin, H., Structure and properties of Co-doped cryptomelane and its enhanced removal of Pb²⁺ and Cr³⁺ from wastewater. *J. Environ. Sci.* **2015**, *34*, 77-85.
28. Healy, T. W.; Herring, A. P.; Fuerstenau, S. W., The effect of crystal structure on the surface properties of a series of manganese oxides. *J. Colloid Interface Sci.* **1966**, *21*, 435-444.
29. Shen, X.; Ding, Y.; Liu, J.; Laubernds, K.; Zerger, R. P.; Polverejan, M.; Son, Y.-C.; Aindow, M.; Suib, S. L., Synthesis, characterization, and catalytic applications of manganese oxide octahedral molecular sieve (OMS) nanowires with a 2×3 tunnel structure. *Chem. Mater.* **2004**, *16*, 5327-5335.
30. Shaughnessy, D. A.; Nitsche, H.; Booth, C. H.; Shuh, D. K.; Waychunas, G. A.; Wilson, R. E.; Gill, H.; Cantrell, K. J.; Serne, R. J., Molecular interfacial reactions between Pu(VI) and manganese oxide minerals manganite and hausmannite. *Environ. Sci. Technol.* **2003**, *37*, 3367-3374.
31. Cornell, R. M.; Giovanoli, R., Transformation of hausmannite into birnessite in alkaline media. *Clays Clay Mineral.* **1988**, *36*, 249-257.